

PAPER

## Local structure and p–d hybridization of Mn-doped $\text{In}_2\text{O}_3$ films

To cite this article: Yukai An *et al* 2012 *J. Phys. D: Appl. Phys.* **45** 295304

View the [article online](#) for updates and enhancements.

### You may also like

- [Effects of Re, Ta, and W \[110\] \(001\) dislocation core of / interface to Ni-based superalloys: First-principles study](#)  
Chuanxi Zhu, , Tao Yu et al.
- [Structural, electronic, and magnetic properties in transition-metal-doped arsenene: Ab initio study](#)  
Min Luo, Yu Hao Shen and Tai Ling Yin
- [Magnetic interactions in a proposed diluted magnetic semiconductor  \$\(\text{Ba}\_{1-x}\text{K}\_x\)\(\text{Zn}\_{1-y}\text{Mn}\_y\)\_2\text{P}\_2\$](#)   
Huan-Cheng Yang, , Kai Liu et al.



**ECS** The Electrochemical Society  
Advancing solid state & electrochemical science & technology

**247th ECS Meeting**  
Montréal, Canada  
May 18-22, 2025  
*Palais des Congrès de Montréal*

**Showcase your science!**

**Abstracts  
due  
December  
6th**

# Local structure and p–d hybridization of Mn-doped $\text{In}_2\text{O}_3$ films

Yukai An<sup>1,3</sup>, Deqiang Feng<sup>1</sup>, Lingshen Duan<sup>1</sup>, Zhonghua Wu<sup>2</sup> and Jiwen Liu<sup>1</sup>

<sup>1</sup> Key Laboratory of Display Materials and Photoelectric Devices, Ministry of Education; Tianjin Key Laboratory for Photoelectric Materials and Devices; School of Material Science and Engineering, Tianjin University of Technology, Tianjin 300384, People's Republic of China

<sup>2</sup> Beijing Synchrotron Radiation Facility (BSRF), Institute of High Energy Physics, Chinese Academy of Sciences, Beijing 100049, People's Republic of China

E-mail: [ayk\\_bj@126.com](mailto:ayk_bj@126.com)

Received 13 April 2012, in final form 11 June 2012

Published 4 July 2012

Online at [stacks.iop.org/JPhysD/45/295304](http://stacks.iop.org/JPhysD/45/295304)

## Abstract

Mn-doped  $\text{In}_2\text{O}_3$  films were deposited on Si (1 0 0) substrates by the RF-magnetron sputtering technique. The influence of Mn-doping concentration on the local structure and degree of p–d hybridization was investigated by x-ray absorption spectroscopy at the Mn K-edge and  $\text{L}_{2,3}$ -edge. The results show that Mn ions dissolve in  $\text{In}_2\text{O}_3$  and substitute for  $\text{In}^{3+}$  sites in the +2 valence states. With the increase in Mn-doping concentration, the Mn–O bonding distance increases monotonically, but integrated intensities of  $\text{L}_{2,3}$  edges increase first and then decrease. It can be concluded that there exists an optimal Mn–O bonding distance for the transition probabilities from the 2p state to the p–d hybridization state, which results in increasing degree of p–d hybridization. So the Mn-doping concentration has a significant effect on the local structure and degree of p–d hybridization in Mn-doped  $\text{In}_2\text{O}_3$  films.

(Some figures may appear in colour only in the online journal)

## 1. Introduction

Over the past few decades, the potential technological applications of diluted magnetic semiconductors (DMSs) to the field of spintronics have triggered extensive studies of many promising systems [1, 2]. Recently, theoretical studies on the basis of Zener's p–d exchange model predicted that a higher  $T_c$  or even a room-temperature DMS can be obtained in wide band gap semiconductors such as ZnO and GaN, doped with transition metals [3, 4].  $\text{In}_2\text{O}_3$  is a technologically important n-type transparent semiconductor with a direct band gap of 3.75 eV and has been widely used as a transparent electrode due to its high mobility ( $10\text{--}75\text{ cm}^2\text{ V}^{-1}\text{ s}^{-1}$ ) with a carrier density of  $10^{19}\text{--}10^{20}\text{ e cm}^{-3}$ . Apparently,  $\text{In}_2\text{O}_3$  is one of the most promising candidates as a host for the development of a ferromagnetic (FM) oxide material. Until now, considerable attention has been paid to the magnetic properties of  $\text{In}_2\text{O}_3$ -based DMS materials fabricated by a variety of methods. It has been reported that  $\text{In}_2\text{O}_3$  doped with

Mn [5], Ni [6, 7], Fe [8–10], Cr [11, 12] and Co [13, 14] exhibits strong room-temperature ferromagnetism. However, the origin of ferromagnetism in this system remains unclear. TM doping in  $\text{In}_2\text{O}_3$  like other oxide DMSs often suffers from the issues related to precipitation of metal clusters or secondary magnetic phases, which are undesirable for practical spintronic applications. On the other hand, for  $\text{In}_2\text{O}_3$ -based DMSs, the ferromagnetism arising from the doped TM atoms can be caused by the interaction between the localized d electrons of magnetic TM impurities and the delocalized host band electrons. Therefore, in order to gain an insight into the origin of ferromagnetism in  $\text{In}_2\text{O}_3$ -based DMSs, the determination of local atomic and electronic structures as well as p–d hybridization of TM atoms inside the  $\text{In}_2\text{O}_3$  lattice is of great importance.

X-ray absorption spectroscopy (XAS) is sensitive to the atomic and electronic structure around the absorbing atom. It involves photoelectrons undergoing transitions from the core state to the unoccupied localized and delocalized states, some of which may be involved in the magnetic cation 3d and

<sup>3</sup> Author to whom any correspondence should be addressed.

anion p-orbital hybridization. So far, rather few XRD studies on Mn-doped  $\text{In}_2\text{O}_3$  have been reported. There is almost no information on how Mn doping induces changes in the local atomic structure and p–d hybridization of the host  $\text{In}_2\text{O}_3$  lattices. In this paper, we report on the local structure and p–d hybridization of Mn-doped  $\text{In}_2\text{O}_3$  films by Mn K-edge and L-edge XAS for the first time, and show the influence of Mn-doping concentration on the local structure and degree of p–d hybridization.

## 2. Experimental details

Mn-doped  $\text{In}_2\text{O}_3$  thin films of about 900 nm thickness were deposited on Si (1 0 0) substrates by RF-magnetron sputtering. The base pressure for the sputtering system was about  $8 \times 10^{-5}$  Pa and all samples were deposited under an Ar (purity 99.999%) pressure of 1.0 Pa. During deposition, the substrate temperature was maintained at 400 °C. An  $\text{In}_2\text{O}_3$  target with some Mn chips symmetrically attached was used to deposit Mn-doped  $\text{In}_2\text{O}_3$  films. By adjusting the number of Mn chips, 4, 5, 8.5 and 13.5 at% Mn-doped  $\text{In}_2\text{O}_3$  films were readily fabricated. The composition of Mn-doped  $\text{In}_2\text{O}_3$  films was determined by x-ray energy dispersive spectroscopy (EDS). The Mn  $L_{2,3}$ -edge XAS spectra were measured by the total electron-yield mode at Beijing Synchrotron Radiation (BSRF) on the 4B9B beamline of x-ray photoemission spectroscopy station. The Mn K-edge x-ray absorption near edge structure (XANES) and extended x-ray absorption fine structure (EXAFS) measurements were carried out at BSRF on the 4B9A beamline of the x-ray diffraction station. These measurements were obtained in the total fluorescence mode. The incident beam was collimated by slits and monochromatized with an Si (1 1 1) double crystal and its intensity was measured by two ionization chambers. Reference spectra of Mn, MnO and  $\text{Mn}_2\text{O}_3$  foils were also measured for comparison and data analysis purposes.

## 3. Results and discussion

In order to determine whether there exist tiny Mn clusters or other Mn oxide secondary phase compounds, we employed the XANES experiments at the Mn K-edge. The XANES technique is a fingerprint of the valence state and neighbour environment of TM cations and is highly sensitive in the investigation of the presence of TM clusters and other impurities in the host matrix. The Mn K-edge XANES spectra of the 4, 5, 8.5 and 13.7 at% Mn-doped  $\text{In}_2\text{O}_3$  films are shown in figure 1. As a guide to the valence state of Mn ions, reference Mn K-edge XANES spectra of standard Mn metal and Mn oxide (MnO and  $\text{Mn}_2\text{O}_3$ ) are also displayed. As is well known, the peak position and the spectral line shape of XANES spectrum strongly depend on the local electronic structure of doped metal ions and, therefore can provide information on the valence state of the absorption atoms in a system. It is clear from figure 1 that the absorption edge positions of all films are very close to the edge of MnO reference, indicating that  $\text{Mn}^{2+}$  ions are dominant in Mn-doped  $\text{In}_2\text{O}_3$  films. However, the XANES spectral features of all films are obviously different

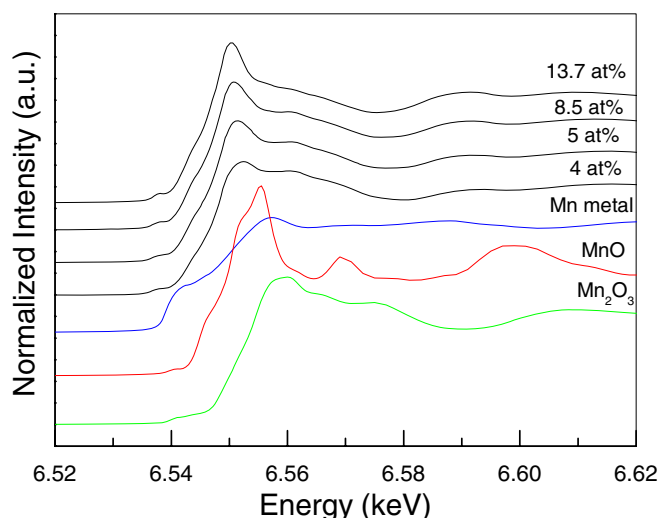


**Figure 1.** Mn K-edge XANES spectra of the 4, 5, 8.5 and 13.7 at% Mn-doped  $\text{In}_2\text{O}_3$  films as well as Mn, MnO and  $\text{Mn}_2\text{O}_3$  foils.

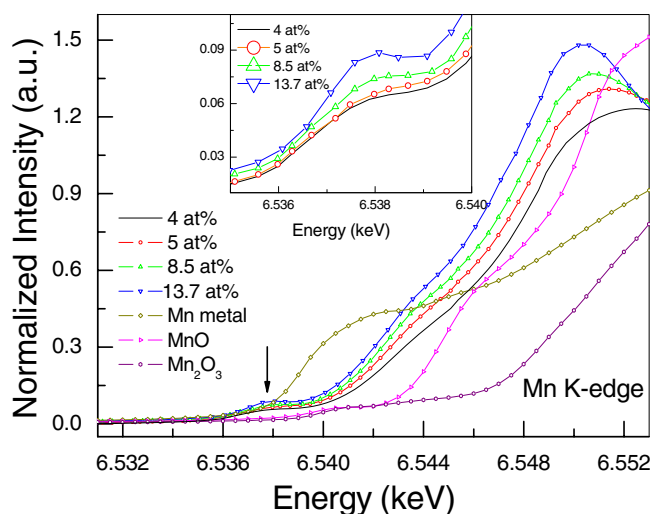


**Figure 2.** Mn K-edge enlarged XANES spectra of the 4, 5, 8.5 and 13.7 at% Mn-doped  $\text{In}_2\text{O}_3$  films as well as Mn, MnO and  $\text{Mn}_2\text{O}_3$  foils.

from those of the standard Mn metal and of MnO or  $\text{Mn}_2\text{O}_3$ . So the existence of Mn metal and Mn oxide can be safely excluded for all Mn-doped  $\text{In}_2\text{O}_3$  films. These indicate a different local structure of Mn for the Mn-doped  $\text{In}_2\text{O}_3$  films; it is possible that all Mn atoms substitute for In atoms in  $\text{In}_2\text{O}_3$ .

Figure 2 shows the Mn K-edge enlarged XANES spectra of the 4, 5, 8.5 and 13.7 at% Mn-doped  $\text{In}_2\text{O}_3$  films as well as Mn, MnO and  $\text{Mn}_2\text{O}_3$  foils. It is noted that there exists a clear pre-edge peak (marked by an arrow in figure 2) around 6.538 keV and a strong white line above the absorption edge, which are also characteristic of  $\text{Mn}^{2+}$  substitution for  $\text{In}^{3+}$  in  $\text{In}_2\text{O}_3$ . From the inset of figure 2, it can be seen that the position of the pre-edge peaks is virtually unchanged, but the intensity remarkably increases with the increase in Mn concentration. The pre-edge absorption peak results from the dipole-forbidden 1s–3d transition and has a significant intensity because of 3d–2p orbital mixing. In general, the pre-edge intensity is mostly influenced by the degree of asymmetry

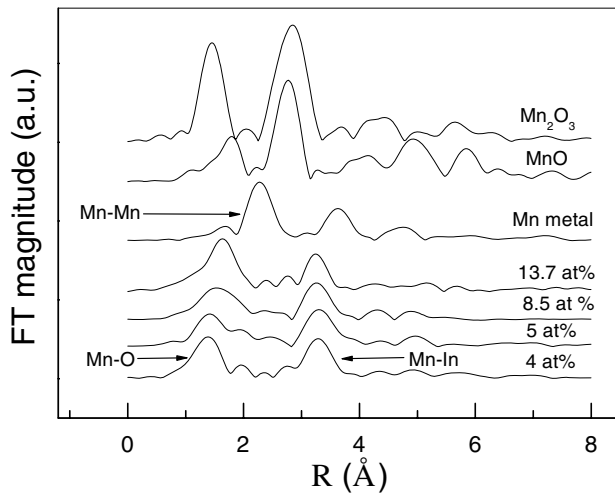


**Figure 3.** Mn K-edge Fourier transforms of the EXAFS spectra of the 4, 5, 8.5 and 13.7 at% Mn-doped  $\text{In}_2\text{O}_3$  films as well as Mn, MnO and  $\text{Mn}_2\text{O}_3$  foils.

and disorder around the central TM ions [15, 16]. Titov *et al* [17] showed that the pre-edge peak is sensitive to the Mn charge state in octahedrally or tetrahedrally coordinated Mn compounds. A single pre-edge peak indicates  $\text{Mn}^{2+}$ , and a double peaked pre-edge peak indicates  $\text{Mn}^{3+}$ . Gautam *et al* [18] showed that the low intensity of the pre-edge peaks refers to centrosymmetric octahedral geometries, whereas the high intensity refers to non-centrosymmetric tetrahedral geometries. So these intensity changes of pre-edge peaks in the spectra of the Mn-doped  $\text{In}_2\text{O}_3$  films suggested that more  $\text{Mn}^{2+}$  ions occupied the tetrahedral sites of the  $\text{In}_2\text{O}_3$  matrix with the increase in Mn concentration.

EXAFS is a powerful technique to investigate local structures around a specific atom and can obtain the distance of nearest neighbours  $R$ . Figure 3 shows the results of Fourier transforms of EXAFS oscillation  $k^3\chi(k)$ , representing the radial distribution function at the Mn K-edge, for the 4, 5, 8.5 and 13.7 at% Mn-doped  $\text{In}_2\text{O}_3$  films as well as standard Mn metal and Mn oxide ( $\text{MnO}$  and  $\text{Mn}_2\text{O}_3$ ). It is clear that there exist two strong peaks at longer radial distance for the 4, 5, 8.5 and 13.7 at% Mn-doped  $\text{In}_2\text{O}_3$  films, suggesting that the local structure around Mn atoms is rather ordered with respect to short range ordering. For the 4 at% and 5 at% Mn-doped  $\text{In}_2\text{O}_3$  films, the two peaks at around 1.44 Å and 3.28 Å are the Mn–O and Mn–In bonding distances, respectively, which correspond to the first and the second nearest neighbour coordination shell. These are completely different from the Mn–Mn bonding distance (2.28 Å) in metal Mn and the Mn–O bonding distance (1.79 Å) in MnO, and are also different from those of  $\text{Mn}_2\text{O}_3$ . So these reveal that Mn ions substituted for  $\text{In}^{3+}$  sites in the Mn-doped  $\text{In}_2\text{O}_3$  films and do not form Mn metal and Mn oxide secondary phases. However, for the 8.5 at% and 13.7 at% Mn-doped  $\text{In}_2\text{O}_3$  films, it can be seen that the peaks of the first Mn–O shell are obviously broadened, and the Mn–O bonding distances slightly increase to 1.54 Å and 1.63 Å, respectively, but those of the second Mn–In shell remain almost unchanged. These indicate that the high Mn-doping concentration can result in more disorder in the first Mn–O shell, but almost does

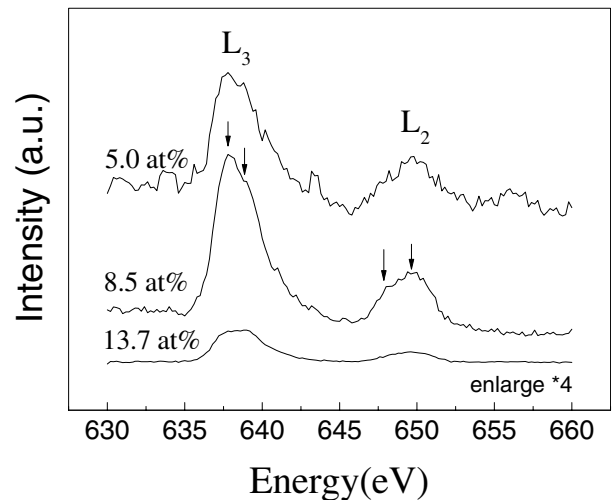


**Figure 4.** Mn L-edge XAS profiles of the 5.0, 8.5 and 13.7 at% Mn-doped  $\text{In}_2\text{O}_3$  films.

not change the neighbour environment of the second Mn–In shell.

Figure 4 shows the Mn  $L_{2,3}$ -edge XAS spectra of the 5, 8.5 and 13.7 at% Mn-doped  $\text{In}_2\text{O}_3$  films. The peak positions and the line shape of the Mn  $L_{2,3}$ -edge XAS spectrum depend on the local electronic structure of the doped Mn ions; it can provide information on the valence state and the ground-state symmetry. From figure 4, it is clear that there exist two main peaks around 638 and 650 eV in the XAS spectra, which correspond to transitions from the Mn  $L_3$  ( $2p_{3/2}$ ) and Mn  $L_2$  ( $2p_{1/2}$ ) states to the continuum of empty 3d states (strictly speaking, transition to a hybridized state of Mn 3d and O 2p). It can also be seen that the  $L_3$  and  $L_2$  edges all exhibit a doublet-peak characteristic (marked by an arrow in figure 4). These features results from Coulomb and exchange interactions of the 2p core holes with the 3d electrons and are typical of localized 3d states. By comparing with the theoretical  $L_{2,3}$ -edge absorption spectra of Mn ion calculated by van der Laan and Kirkman [19], Mn  $L_{2,3}$ -edge XAS spectra of the Mn-doped  $\text{In}_2\text{O}_3$  films have a similar profile to that of the Mn  $d^5$  ground state with the crystal field strength 0.5 eV. These further suggest that most of the Mn atoms in our Mn-doped  $\text{In}_2\text{O}_3$  films are bivalent ( $\text{Mn}^{2+}$ ).

As is well known, Mn doping in  $\text{In}_2\text{O}_3$  films can result in the hybridization between the Mn 3d and O 2p orbitals. So the  $L_3$  and  $L_2$  edges are attributed to photoelectron transitions from the Mn  $2p_{1/2}$  and  $2p_{3/2}$  states to the final unoccupied Mn 3d–O 2p hybridized electron states. The integrated intensities of Mn XAS spectra at  $L_3$  and  $L_2$  edges can also reflect the total numbers of Mn  $2p_{3/2}$  and  $2p_{1/2}$  to Mn 3d–O 2p hybridized state transitions, respectively. For  $L_3$ -edge absorption, a multiple-peak Gaussian fitting is used due to its doublet-peak structure. It can be seen from figure 5 that the  $L_3$ -edge spectrum of the 8.5 at% Mn-doped  $\text{In}_2\text{O}_3$  films can be fitted by three peaks I, II and III. Peaks III can be attributed to photoelectron transitions from the Mn  $2p_{3/2}$  states to the 4s states in the conduction band [20]. It should be excluded from the integrated intensity due to no contribution to the p–d hybridization. The inset of figure 5 shows the Mn  $L_3$ -edge XAS profiles of the 5.0, 8.5 and



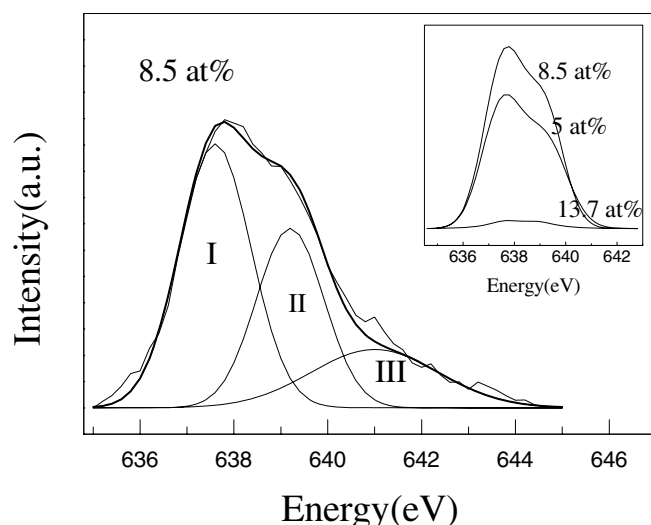


**Figure 5.** Mn  $L_3$ -edge XAS profiles fitted by three peaks I, II and III of the 8.5 at% Mn-doped  $\text{In}_2\text{O}_3$  films. The inset shows Mn  $L_3$ -edge XAS profiles without including peak III, for the 5.0, 8.5 and 13.7 at% Mn-doped  $\text{In}_2\text{O}_3$  films.

13.7 at% Mn-doped  $\text{In}_2\text{O}_3$  films without including peak III. It is obvious that the integrated intensity first increases with the increase in Mn concentration, then obviously decreases for the 13.7 at% Mn-doped  $\text{In}_2\text{O}_3$  films, namely  $I_{8.5\text{ at\%}} > I_{5\text{ at\%}} > I_{13.7\text{ at\%}}$ . The same change trend is also found for the  $L_2$  edge absorption.

It is interesting that the integrated intensities for both  $L_3$  and  $L_2$  edges do not increase monotonically with the increase in Mn concentration. As is well known, the overlap degree of p and d orbital wave functions decides the strength of p–d hybridization as well as the transition probabilities from the 2p state to the p–d hybridization state. So it can be considered that under low doping concentrations, only a few Mn atoms are incorporated into the  $\text{In}_2\text{O}_3$  lattice and occupy the In sites, which results in the fact that the integrated intensity is small. With a further increase in Mn-doping concentration, more Mn atoms are incorporated into the  $\text{In}_2\text{O}_3$  lattice and substitute for In atoms, which results in more Mn 3d orbitals becoming available for hybridization with O 2p orbitals. So the strength of p–d hybridization will be higher and the integrated intensity also increases. However, when the Mn-doping concentration increases to 13.7 at%, the integrated intensity remarkably decreases. According to the EXAFS results, the existence of Mn metal and Mn oxide secondary phases in the films can be safely excluded and the Mn–O bonding distance increases with the increase in Mn concentration, namely  $R_{5\text{ at\%}} (1.44 \text{ \AA}) < R_{8.5\text{ at\%}} (1.54 \text{ \AA}) < R_{13.7\text{ at\%}} (1.63 \text{ \AA})$ . So the decrease in integrated intensity in the 13.7 at% Mn-doped  $\text{In}_2\text{O}_3$  film does not result from the Mn-related secondary phases. It is possible that there exists an optimal Mn–O bonding distance for the transition probabilities from the 2p state to the p–d hybridization state, which results in the increase in the integrated intensity. When the Mn–O bonding distance further increases, the overlap degree of p and d orbital wave functions is decreased. Then, the strength of p–d hybridization becomes low and the overall number of Mn

2p<sub>3/2</sub> and 2p<sub>1/2</sub> to Mn 3d–O 2p hybridized states' transition also decreases for the higher doping concentration.

According to Zener's p–d exchange model, the Mn 3d orbit hybridized with the O 2p orbit at the Fermi level in the band gap and a strong p–d interaction can lead to a FM coupling between two Mn ions connected by an intervening O atom, namely Mn–O<sup>2−</sup>–Mn groups. The magnetic moment is very sensitive to the Mn–O bonding distance that makes Mn-based oxide DMSs exhibit very complicated magnetic properties ranging from FM to antiferromagnetic or nonmagnetic. Zhang *et al* [21] predicted that the FM coupling can be strongly affected by the Mn–O bond length in  $\text{La}_{0.67}\text{Ca}_{0.33}\text{MnO}_3$  films. Spaldin [22] found that the energy differences between FM and antiferromagnetic alignment are very small in a Co-doped ZnO system and a slight change in the Co–O bonding distance can result in a change in the FM or antiferromagnetic coupling. Coey *et al* [23] proposed a FM exchange mechanism involving oxygen vacancies ( $\text{V}_\text{O}$ ), which form F-centres with trapped electrons. Overlap of the F-centre electron orbital with the d orbital of the neighbouring Mn spins to form Mn– $\text{V}_\text{O}$ –Mn groups is also important for the FM coupling. So it can be concluded that the Mn-doping concentration has a significant effect on the degree of p–d hybridization and the FM coupling in Mn-doped  $\text{In}_2\text{O}_3$  films. However, further experimental and theoretical analyses of the correlation among the oxygen vacancies, Mn–O bond length and magnetic properties are needed to address this issue.

## 4. Conclusion

In summary, we have prepared Mn-doped  $\text{In}_2\text{O}_3$  films with different Mn-doping concentrations by the RF-magnetron sputtering technique. The local structure and p–d hybridization of Mn were investigated by the XAS technique. The Mn K-edge and  $L_{2,3}$ -edge XAS measurements indicate that  $\text{Mn}^{2+}$  ions substitute for  $\text{In}^{3+}$  without changing the bixbyite cubic structure of  $\text{In}_2\text{O}_3$ . With the increase in Mn concentration, the Mn–O bonding distance increases monotonically, but the integrated intensities of both  $L_3$  and  $L_2$  edges increase first and then decrease. It may be due to the existence of an optimal Mn–O bonding distance for the transition probabilities from the 2p state to the p–d hybridization state. So the Mn-doping concentration has a significant effect on the local structure and degree of p–d hybridization in Mn-doped  $\text{In}_2\text{O}_3$  films.

## Acknowledgments

This work was supported by the National Natural Science Foundation of China (Grant No 10904110 and 11174217) and the Tianjin Natural Science Foundation of china (Grant No 10JCYBJC01600) and by the Beijing Synchrotron Radiation Laboratory.

## References

- [1] Ando K 2006 *Science* **312** 1883
- [2] Ohno H 1998 *Science* **281** 951
- [3] Dietl T, Ohno H, Matsukura F, Cibert J and Ferrand D 2000 *Science* **287** 1019

- [4] Dietl T, Ohno H and Matsukura F 2001 *Phys. Rev. B* **63** 195205
- [5] Philip J, Theodoropoulou N, Berera G, Moodera J S and Satpati B 2004 *Appl. Phys. Lett.* **85** 777
- [6] Hong N H, Sakai J, Huong N T and Brize V 2005 *Appl. Phys. Lett.* **87** 102505
- [7] Hong N H, Sakai J, Huong N T and Brize V 2006 *J. Magn. Mater.* **302** 228
- [8] Jiang F X *et al* 2011 *J. Appl. Phys.* **109** 053907
- [9] Xu X H *et al* 2009 *Appl. Phys. Lett.* **94** 212510
- [10] Xing P F *et al* 2008 *Appl. Phys. Lett.* **92** 022513
- [11] Hsu C Y 2011 *J. Phys. D: Appl. Phys.* **44** 415303
- [12] Kharel P *et al* 2007 *J. Appl. Phys.* **101** 09H117
- [13] Meng X Q, Tang L M and Li J B 2010 *J. Phys. Chem. C* **114** 17569
- [14] Hakimi A M H R *et al* 2011 *Phys. Rev. B* **84** 085201
- [15] Westre T E *et al* 1997 *J. Am. Chem. Soc.* **119** 6297
- [16] Li G G, Bridges F and Booth C H 1995 *Phys. Rev. B* **52** 6332
- [17] Titov A *et al* 2005 *Phys. Rev. B* **72** 115209
- [18] Gautam S *et al* 2009 *J. Phys. D: Appl. Phys.* **42** 175406
- [19] van der Laan G and Kirkman I W 1992 *J. Phys.: Condens. Matter* **4** 4189
- [20] Kao J K, Hsieh H H, Pieh J Y, Chang Y K, Kou K C and Tseng P K 1997 *Phys. Rev. B* **55** 7633
- [21] Zhang W *et al* 1998 *Phys. Rev. B* **58** 14143
- [22] Spaldin N A 2004 *Phys. Rev. B* **69** 125201
- [23] Coey J M D *et al* 2004 *Appl. Phys. Lett.* **84** 1332
- Coey J M D, Venkatesan M and Fitzgerald C B 2005 *Nature Mater* **4** 173